Journal of King Saud University – Science (2017) 29, 371–379

King Saud University
Journal of King Saud University – Science
www.ksu.edu.sa
www.sciencedirect.com

# Evaluation of the dosimetric characteristics of 6 MV flattened and unflattened photon beam

Maged Mohammed [a,b,*], E. Chakir [a], H. Boukhal [b], S. Mroan [b], T. El Bardouni [b]

[a] SIMO-LAB, Faculty of Sciences, Ibn Tofail University, Kenitra, Morocco
[b] Radiations and Nuclear Systems Laboratory, University Abdelmalek Essaadi, Faculty of Sciences, Tetouan, Morocco

Received 4 August 2016; accepted 25 September 2016
Available online 30 September 2016

**KEYWORDS**

Flattening filter;
Monte Carlo;
Dosimetric properties;
Varian

**Abstract** This work aims to compare and evaluate the dosimetric properties of 6 MV flattening (FF) and flattening filter free (FFF) photon beams which generated from a Varian 2100 medical accelerator. These properties include percentage depth dose, dose rate, beam profile, out-of-field, energy spectra, scatter factor, and surface dose. This study has been effected by using BEAMnrc and DOSXYZnrc user's code based on EGSnrc Monte Carlo method.

The results obtained showed that the unflattened beams have a dose rate of 2.46 times higher than the flattened beams that would reduce the treatment time. The out-of-field dose of FFF beams at 3.5 cm from the field edge was less than the flattened one due to the reduction of head scatter. The scatter factor and penumbra dose of unflattened beam were found less than that of the flattened one for all field sizes. The unflattened beam has a higher surface dose and build-up dose compared to the flattened beams. Replacing the air column under the jaws by helium leads to the reduction of the surface dose ratio from 1.23 to 1.13, build-up doses and $d_{max}$ restored as in flattened case. The results of this study have demonstrated that, unflattened beams are very useful for treating cancer cells and sparing the adjacent healthy tissue.


## 1. Introduction

Generally, in conventional radiotherapy, the flattening filter (FF) was one of the basic components in the treatment head of a medical accelerator which is located between the primary collimator and the ion chamber. The flattening filter has been introduced in the treatment head of a medical accelerator, which results in an almost uniform dose at a certain depth and to flat the photon beams generated by the bremsstrahlung phenomenon, which have a conical shape profile. The FF is composed of high Z material and usually has a bell-shape (Georg et al., 2011; Lutz and Larsen, 1984).

Recently, depending on several studies of the dosimetric properties of unflattened beams, many types of Linacs have been made without the flattening filter (FFF), particularly, with those using more intense and conformal irradiations such

* Corresponding author at: SIMO-LAB, Faculty of Sciences, Ibn Tofail University, Kenitra, Morocco.
E-mail address: magedm22@gmail.com (M. Mohammed).
Peer review under responsibility of King Saud University.

Production and hosting by Elsevier

http://dx.doi.org/10.1016/j.jksus.2016.09.008

as (IMRT), (SPRT) and others, high dose rate required (Mesbahi, 2007; Pichandi et al., 2014).

Several studies have been conducted on different energies 6, 8, 10, 15 and 18 MV to assess the dosimetric characteristics of flattening filter free (FFF) as (Chung et al., 2015; Detappe et al., 2013; Georg et al., 2011; Kragl et al., 2009; Kry et al., 2007; Mesbahi, 2007; Najem et al., 2014; Pichandi et al., 2014; Tsiamas et al., 2014; Wang et al., 2012), they reported that removing the filter increases the dose rate and reduces the head scatter, neutrons contamination, out-of-field and penumbra doses. They concluded that unflattened beams possesses high efficiency compared to flattened beams. On the other hand FFF beams have surface and build-up doses more than that of flattening beams, but its impact is not significant for patient safety.

In this current study, the dosimetric properties of 6 MV flattened (FF) and unflattened photon beams have been investigated using EGSnrc Monte Carlo method.

## 2. Materials and method

A 6 MV photon beam of Varian 2100 medical accelerator was studied using EGSnrc Monte Carlo method. The measurements data and alinac head geometry including the target, primary collimator, flattening filter, and jaws have been provided by the manufacturer (Varian Medical Systems, Palo Alto, CA, USA). All the measured data were acquired in water phantom of volume $40 \times 40 \times 40\ cm^3$, and the measurements were obtained at a source-to-surface distance (SSD) of 100 cm.

### 2.1. Monte Carlo simulations

The EGSnrc-based user codes BEAMnrc (Rogers et al., 2001) and DOSXYZnrc (Walters et al., 2005) have been used to perform the simulation of 6 MV with and without flattening filter photon beams.

BEAMnrc user code was used to model the linac's head and to simulate the photon beams. The phase space files, that were located at $Z = 100$ cm from the target, were generated.

Variance reduction techniques were applied: as the photon and electron cut-off energies were set to 10 keV (PCUT) and 711 keV (ECUT), respectively. Electron range rejection was set to 1 MeV (ESAVE). The threshold for secondary particle production was set to ECUT for charged particles and PCUT for photons. Directional bremsstrahlung splitting (DBS) was used with a splitting number of 100, SSD = 100, field size = 10 and Russian roulette turned off. EGSnrc parameters were set as default. For all simulations $6 \times 10^6$ histories were run.

Secondly, the dose distributions were calculated by DOSXYZ user code in a homogenous water phantom, placed at 100 cm from the target, of $40 \times 40 \times 40\ cm^3$. Non-uniform voxels have been defined. In this step a phase space file which is generated by BEAMnrc user code, and fixed at the isocentre level, will be used as a source of particles in DOSXYZ.

EGSnrc parameters were set as default. Electron range rejection was set to 1 MeV (ESAVE). A $4 \times 10^8$ histories were used for each simulation.

Other beam characteristics such as mean energy, energy spectra, distribution angular and others, were obtained when phase space files were analyzed by BEAMDP (Ma and Rogers, 2004) user code.

### 2.2. Monte Carlo validation

Before studying the dosimetric properties of both flattened and unflattened photon beams, the optimum parameters of the incident electron must be selected, such as mean energy and beam width. For this purpose, the dose distribution (percentage depth dose (PDD) and beam profile) was calculated and compared to the experimental data, using gamma index criteria. The simulations were carried out for square field sizes of $3 \times 3$, $10 \times 10$ and $20 \times 20\ cm^2$ in a homogenous water phantom of $40 \times 40 \times 40\ cm^3$, which were recommended from the manufacturer, placed at SSD = 100 cm.

### 2.3. Dosimetric proprieties calculations

After selecting the optimum electron parameters, the characteristics of with and without flattening filter photon beams such as PDDs, beam profile and energy spectra were investigated.

### 2.4. Surface dose and build-up

Surface dose or skin dose is the dose calculated at the skin or the entrance of the phantom. It is still clinically important thank to the knowledge of the build-up effect which can facilitate the preservation of skin sparing or the delivery of an adequate dose to superficial target volumes (Wang et al., 2012). In our previous study for 12 MV photon beams (Maged Mohammed et al., 2015), we found that the surface dose and build-up region doses are affected by field size, energy and SSD. In this present work, the surface dose of 6MV FF and FFF configurations was evaluated for $3 \times 3$, $6 \times 6$, $15 \times 15$, $10 \times 10$ and $20 \times 20\ cm^2$ open field sizes.

### 2.5. PDDs, $d_{max}$ and dose rate

The PDDs curves for FF and FFF beams were calculated in the central axis of a homogenous water phantom. The depth of maximum dose ranges from 0 to 5 cm for orthovoltage X-ray to 25 MV photon beams (Pichandi et al., 2014). It depends on the energy and field size. The dose rate ratio of flattened and unflattened beams is calculated at a depth of 10 cm.

### 2.6. Beam profiles and out-of-field

Lateral beam profiles of both FF and FFF beams of different field sizes were evaluated at a depth of 10 cm. Beam profiles were normalized to the dose at central axis. The difference of out-of-field doses was calculated at 3 cm from the field edge.

## 3. Results and discussion

The statistical uncertainty of our calculation was less than 0.6% for all points in PDDs curves, and for beam profile, it was less than 0.6% inside the field, 0.9% in penumbra region and 1.4% out-off field.

### 3.1. MC validation

To validate the MC model, the PDDs and lateral profile curves which were calculated in a homogenous water phantom were compared with experimental data that were provided by the manufacturer. PDDs curves were normalized to maximum dose and beam profile to the dose on the central axis at 10 cm depth. The Fig. 1 shows the comparisons of dose distribution calculated and measured. For selecting the mean energy, the group with energy from 5.5 to 6.5 MeV with step of 0.1 MeV was tested on all field sizes and the beam width set to 0.2 mm.

After selecting the optimal mean energy value, a full width half mean (FWHM) of the electron incident from 0.1 to 3 mm with step of 0.1 mm was tested.

About 60 simulations were carried out for tuning the electrons incidents parameters, in each simulation our results were compared with experimental data using gamma index criteria. The statistical uncertainty in each simulation was less than 0.4% and it was less than 1% in out-off field dose. Depending on the Gamma index analysis, a match between measurement and simulation was found for an incident electron beam with a mean energy of 5.7 MeV and a focal spot size was 1.6 mm (FWHM). The agreement between MC calculations and

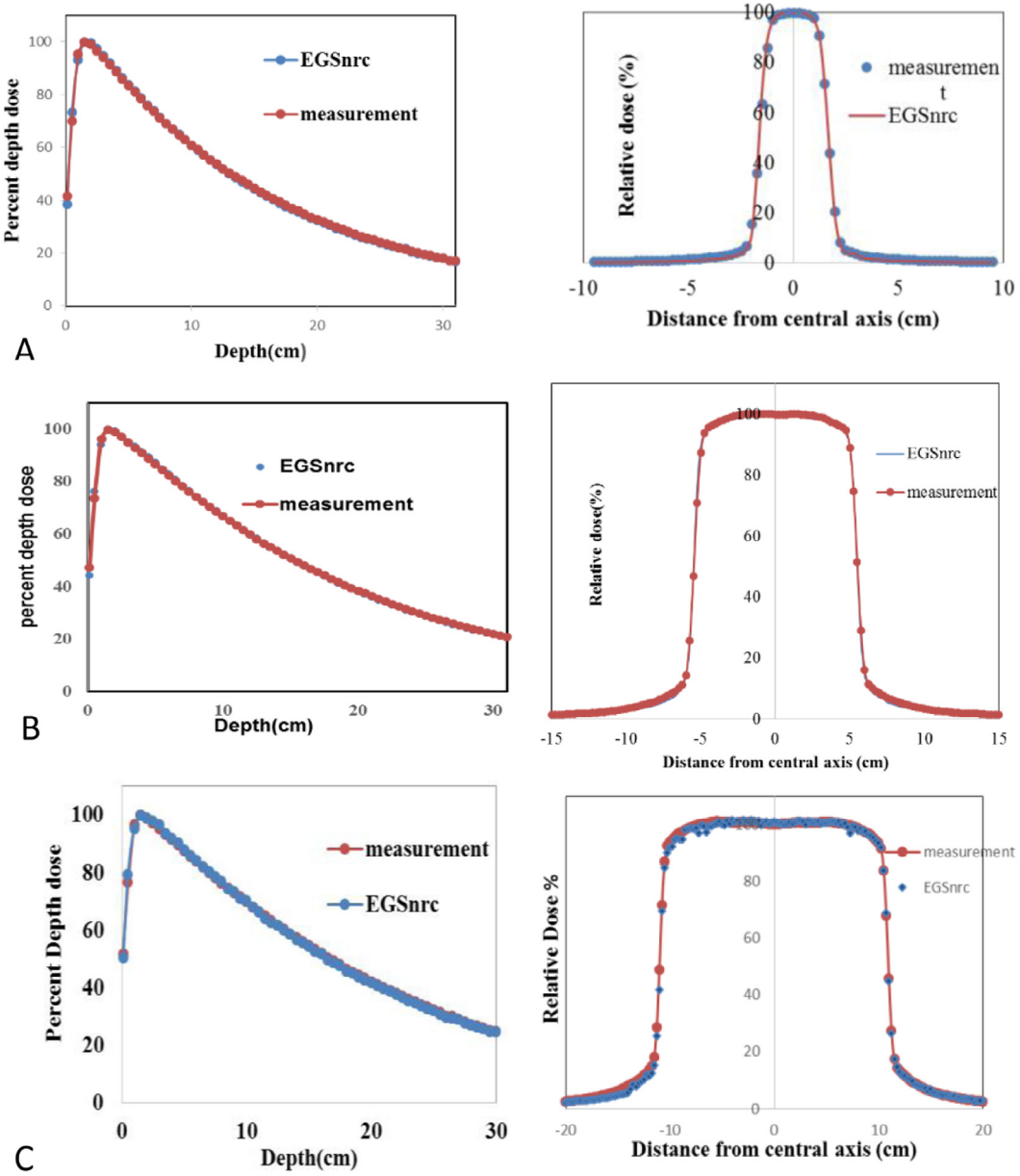


**Figure 1** A comparison of measured and calculated PDDs and beam profile curves of the 6 MV photon beam for: (A) 3 × 3, (B) 10 × 10 and (C) 20 × 20 $cm^2$ field sizes.

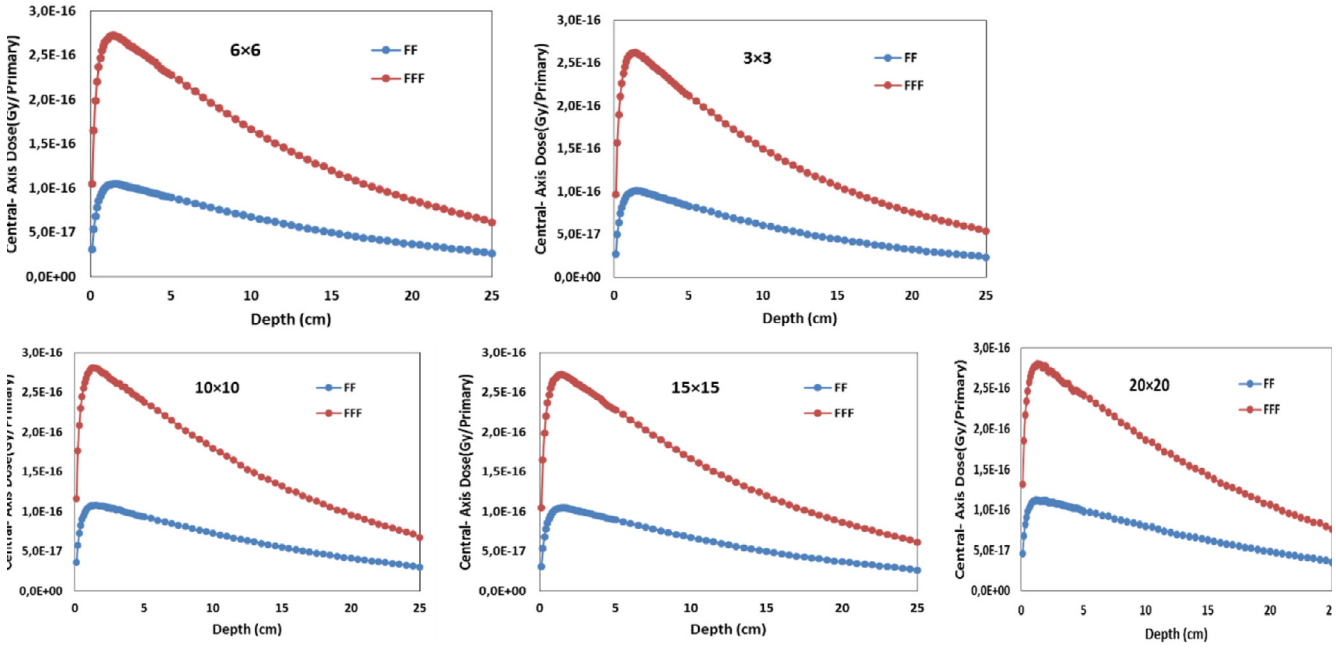


**Figure 2** Comparisons of the central axis depth dose per primary particles of FF and FFF beams for 3 × 3, 6 × 6, 15 × 15, 10 × 10 and 20 × 20 $cm^2$ field sizes.

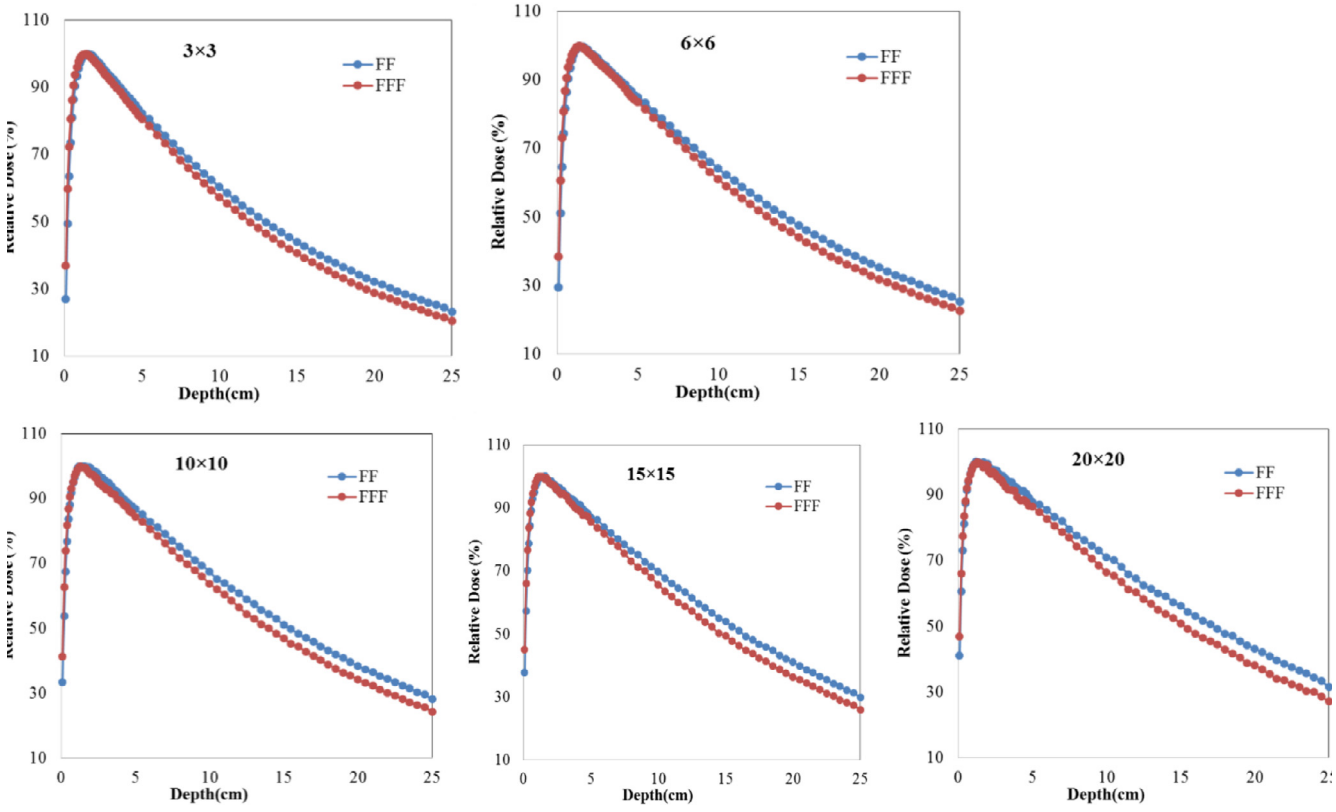


**Figure 3** Percentage depth doses of the unflattened and flattened photon beams by measurements and Monte Carlo simulations in water phantom for 3 × 3, 6 × 6, 15 × 15, 10 × 10 and 20 × 20 $cm^2$ field sizes.

measurements was within 1.5% for depth dose curves and within 2% for beam profiles. The results of the present work were compatible with the study of Hrbacek et al. (2011), Mesbahi et al. (2006) and Wiant et al. (2013).

**Table 1** $D_{20}/D_{10}$ ratios for different field seizes.

| Field size ($cm^2$) | FF | FFF |
|---|---|---|
| 3 × 3 | 0.53 | 0.50 |
| 6 × 6 | 0.55 | 0.52 |
| 10 × 10 | 0.569 | 0.54 |
| 15 × 15 | 0.588 | 0.55 |
| 20 × 20 | 0.607 | 0.57 |

**Table 2** Summary of surface doses for 6 MV flattened and unflattened photons and the ratio between them.

| Field size ($cm^2$) | FF | FFF | Ratio of FFF and FF |
|---|---|---|---|
| 3 × 3 | 26.8 | 36.8 | 1.37 |
| 6 × 6 | 29.36 | 38.4 | 1.309 |
| 10 × 10 | 33.43 | 41.2 | 1.233 |
| 15 × 15 | 37.7 | 45.06 | 1.195 |
| 20 × 20 | 41.04 | 46.85 | 1.141 |

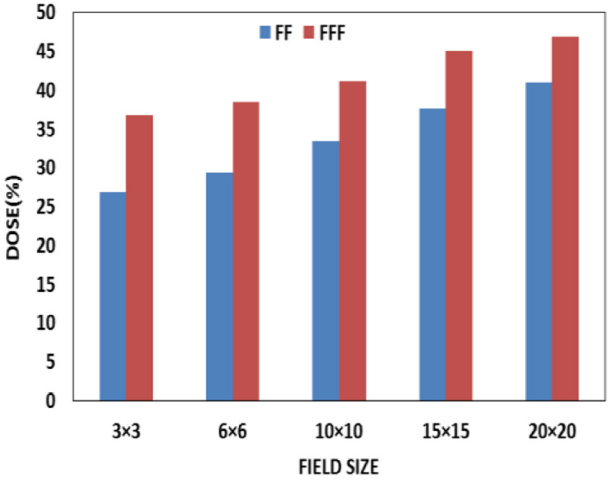


**Figure 4** Surface doses comparisons of 6MV FF and FFF photon beam calculated at 1 mm within the water phantom.

### 3.2. Dose rate

The data presented in Fig.2 shows the central – axis depth absorbed-dose distribution per primary particles of both configurations of FFF and FF beams in a homogenous water phantom for 3 × 3, 6 × 6, 15 × 15, 10 × 10 and 20 × 20 $cm^2$ field sizes. The dose rate of FFF was found to be 2.46 times higher than that for the flattened beams. This value was obtained on the central axis dose at a depth 10 cm and SSD = 100 cm. The present study reports a difference less than 0.15 compared with the findings of Mesbahi (2007) and Vassiliev et al. (2006), the difference owing to the filter material. Studies have reported that the dose rate increases on the central axis by more than a factor of 2 compared to irradiation with the FF beams (Titt et al., 2006). The results reported in the present paper seem convergent with the findings of Titt et al. (2006) for a 6 MV photon beam. The increase in dose rate in FFF configuration due to the flattening filter eliminates a large part of the primary photons from the beam center, especially close to the central axis, and a greater number of primary photons will be attenuated. The increase in dose rate is one of the advantages of removing the flattening filter, this feature may offer an improvement in the treatment of cancer or this can lead to reduction in the irradiation time per treatment fraction (Titt et al., 2006). Reducing the delivery time will benefit some motion control techniques, such as breath-hold and mostly for treatment of small field sizes (Xiao et al., 2015). The higher dose rates improve treatment delivery efficiency and there are no radiobiological correction factors that need to be considered when using unflattened beams (Georg et al., 2011). Previous studies report usefulness of FFF beams compared with FF beams but caution is needed for accurate measurements and better planning to protect the cells health.

### 3.3. PDDs at the central axis

The percentage depth dose curves, of both configurations FF and FFF were calculated on the central axis of a homogenous water phantom placed at 100 cm from the source. The Fig. 3 illustrates the simulation results obtained for open field sizes from 3 × 3 to 20 × 20 $cm^2$. It can be seen that after the maximum dose, unflattening beams have a steep downward movement with depth compared to flattened beams. Due to the softness energy spectrum, we found that a large part of FFF beams energy was deposited to a build-up region compared to the depth more than $d_{max}$. Through Fig. 3, it can be seen that the spacing between two curves increases with field size. This effect quantified by using the ratio of the dose in 20 cm to 10 cm depth ($D_{20}/D_{10}$). This ratio is summarized in Table 1 and, it was consistent with that reported by Kragl et al. (2009) in this work, we found that the unflattened beam energy of 10 × 10 $cm^2$ field size (%dd at 10 cm) decreased from 67.4% to 63.7%. Vassiliev et al. (2006) found that PDD of unflat-

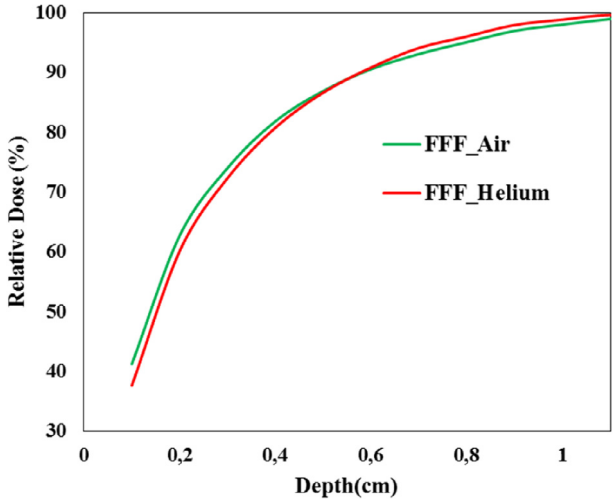


**Figure 5** Build-up doses of 6MV unflattened beam for both air and Helium molecules.

tened 6 MV beams was corresponding to standard 4 MV beams.

Analyzing the phase space files of both FF and FFF beams shows that the number of electrons in FFF phase space was more than twice of FF one. The replacement of the air column, under the jaws to the phantom surface, by helium leads to the reduction of the electron contamination due to many of the electrons created when the radiation interacts with the air molecules. In FFF simulation case, the same number of electrons was recorded compared to standard flattened beams when the simulations were carried out with helium molecules.

### 3.4. Surface dose and build-up region

The surface dose and build-up region of FF and FFF photon beams were evaluated for $3 \times 3$ to $20 \times 20\ cm^2$ square field sizes. The surface dose value of any field size is defined as the dose calculated at the first millimeter (1 mm) of a homogeneous water phantom divided by the dose at $D_{max}$ for the corresponding field. Simulation results summarized in Table 2 show that the surface dose increased linearly with field size for both FF and FFF photon beams. The surface dose values of FFF beams were higher than that of the FF for all field sizes, due to the increasing of incident contaminant charged particles and low energy photons in FFF beams (Mesbahi, 2007; Titt et al., 2006; Vassiliev et al., 2006; Wang et al., 2012). The difference between them is clear in the Fig. 4. The surface dose ratios of FFF and FF beams decrease with field size due to an increasing of scattering radiation from the filter with field size. The results reported in the present paper seem convergent with the findings of Vassiliev et al. (2006) and Yarahmadi et al. (2013), with a slight disparity (about 0.04) because they calculated it at 3 mm (present work at 1 mm). Using helium molecules decreased the ratio from 1.233 to 1.13 for $10 \times 10\ cm^2$ field size, and there is a decrease in build-up region doses, as seen in Fig. 5. The build-up region

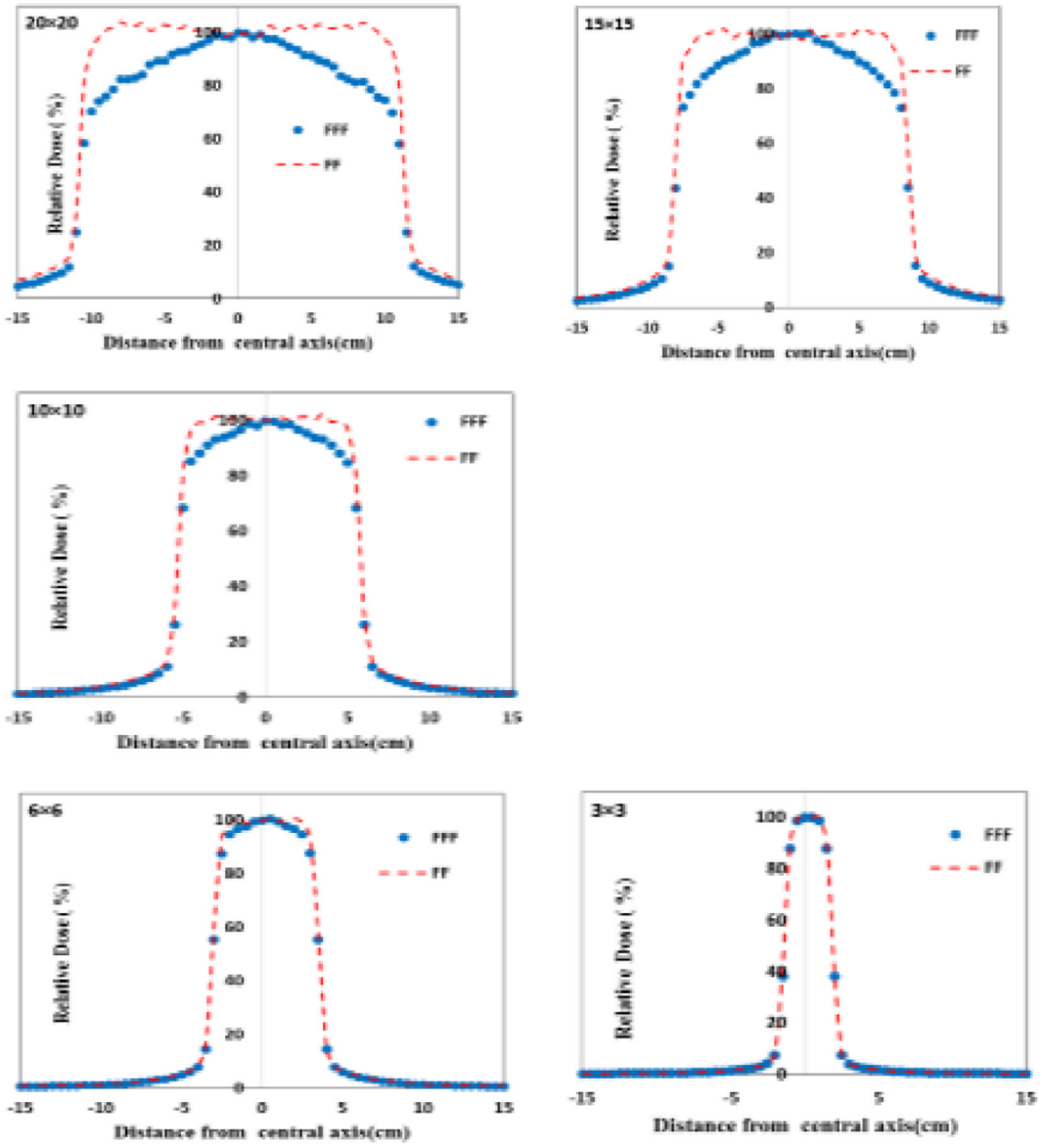


**Figure 6** Comparison of beam profiles of FF and FFF 6 MV photon beams for different field sizes.

**Table 3** Ratios of maximum and minimum dose inside the field (within 80% of the field size) for field sizes from 3 × 3 to 20 × 20 $cm^2$ calculated at a depth of 10 cm.

| Field size ($cm^2$) | FF | FFF |
|---|---|---|
| 3 × 3 | 1.01 | 1.01 |
| 6 × 6 | 1.01 | 1.057 |
| 10 × 10 | 1.01 | 1.13 |
| 15 × 15 | 1.01 | 1.28 |
| 20 × 20 | 1.01 | 1.32 |

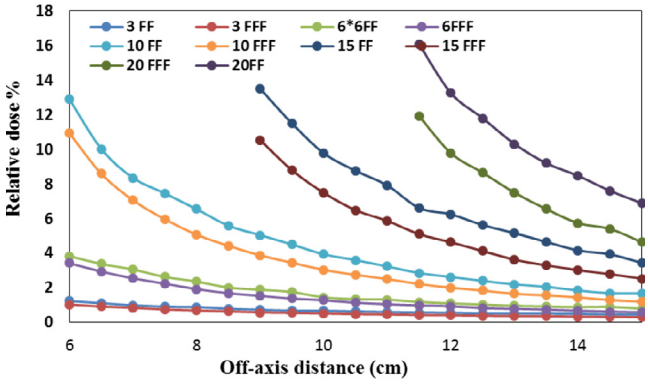


**Figure 7** Comparison of out-of-field dose of FF and FFF 6 MV photon beams for different field sizes.

dose (depth, from 0 to $d_{max}$) for FFF configuration is larger than that of FF configuration for open field sizes from 3 × 3 to 20 × 20 $cm^2$. Our results are consistent with that obtained in the previous study of Wang et al. (2012). They concluded that, the difference is not substantial and can be clinically insignificant. Sigamani et al. (2016) and Wang et al. (2012) reported that the dose delivered to surface dose and build-up region is useful for implementations of IMRT, SRS, and SBRT techniques. Using helium particles play an efficient role by increasing the efficiency and quality of unflattened beams and the patients would benefit considerably from the reduction in surface dose.

### 3.5. Beam profiles

Fig. 6 shows the lateral profiles dose, of both FF and FFF beams for the open field size from 3 × 3 to 20 × 20 $cm^2$, that is calculated at a depth of 10 cm. From Fig. 6, we can see clearly the lack of flatness feature in FFF beams that have their maximum dose on the central axis and decrease gradually toward the field edge. This shape becomes more pronounced with increasing of field size and beam energy (Hrbacek et al., 2011). This behavior is quantified by calculating the ratio of maximum and minimum dose on the central axis (within 80% of the field size), and summarizes in Table 3. We can see that for a field up to 3 × 3 $cm^2$ this ratio increases with field size, Table 3.

The obtained results show that removing the filter leads to the reduction of the penumbra dose. We found that the average ratios of FF and FFF in the penumbra region were obtained from 1.04 to 1.33 for 3 × 3 to 20 × 20 $cm^2$ field sizes, respectively. At the same time, smaller penumbra width was produced due to the softer beam spectrum of FFF and missing scatter from the flattening filter (Pönisch et al., 2006).

Out-of-field doses of flattened and non-flattened beams were assessed for square filed sizes from 3 × 3 to 20 × 20 $cm^2$, in beam profiles which were calculated at a depth of 10 cm. From the Figs. 6 and 7, it is clear that the removal of the filter produces lower dose outside treatment field due to the reduction of leakage radiation and head scatter (Georg et al., 2011), the difference between FFF and FF doses in outside the field (at 3.5 cm from the treatment field border) were 40%, 35%, 31%, 20% and 15% for 20 × 20, 15 × 15, 10 × 10,6 × 6 and 3 × 3 $cm^2$ field sizes, respectively. The difference is more accentuated with large field size, Fig. 7, because of more collimator scatter with flattened beams. In clinical situations, the dose outside the cancer will be influenced by many parameters such as size, location, and shape of the target as well as degree of modulation and delivery technique used (intensity-modulated radiotherapy or volumetric modulated arc therapy) and their interplay with beam characteristics. In a previous study of Diallo et al. (2009) reported that 49% of the secondary cancer occurs at the field edge. Based on the results of this work, the best possible dose reduction outside the field was achieved with FFF beams. This reduces the damage on healthy tissues close the target.

### 3.6. Total scatter factor (Sc,p)

It's the ratio of the dose at a reference depth in a water phantom for a given field size to the dose at the corresponding point and depth in a phantom for the reference field size (10 × 10 $cm^2$) for FF and FFF beams (Smathers, 2003).

Sc values of FF and FFF photon beams were calculated at depth of 10 cm for different field sizes. The results obtained are presented in Table 4. The previous study of (Georg et al., 2011; Hrbacek et al., 2011; Pichandi et al., 2014; Vassiliev et al., 2006) has consistent results, and reported that the flattening filter is one of the components which contribute to the dispersion of the number of particles. So, the removal of filter reduces the dose outside the region of interest, and the organs besides the cancer arebetter protected.

### 3.7. Photon energy spectra

Photon energy spectra of each field size were evaluated by analyzing the phase space files which were placed at the water phantom surface ($Z$ = 100 cm) using BEAMDP user code.

**Table 4** Summarized of head scatter for FFF and FF beams.

| Field size ($cm^2$) | FF | FFF |
|---|---|---|
| 3 × 3 | 0.838 | 0.837 |
| 6 × 6 | 0.929 | 0.927 |
| 10 × 10 | 1.00 | 1.00 |
| 15 × 15 | 1.07 | 1.05 |
| 20 × 20 | 1.09 | 1.04 |

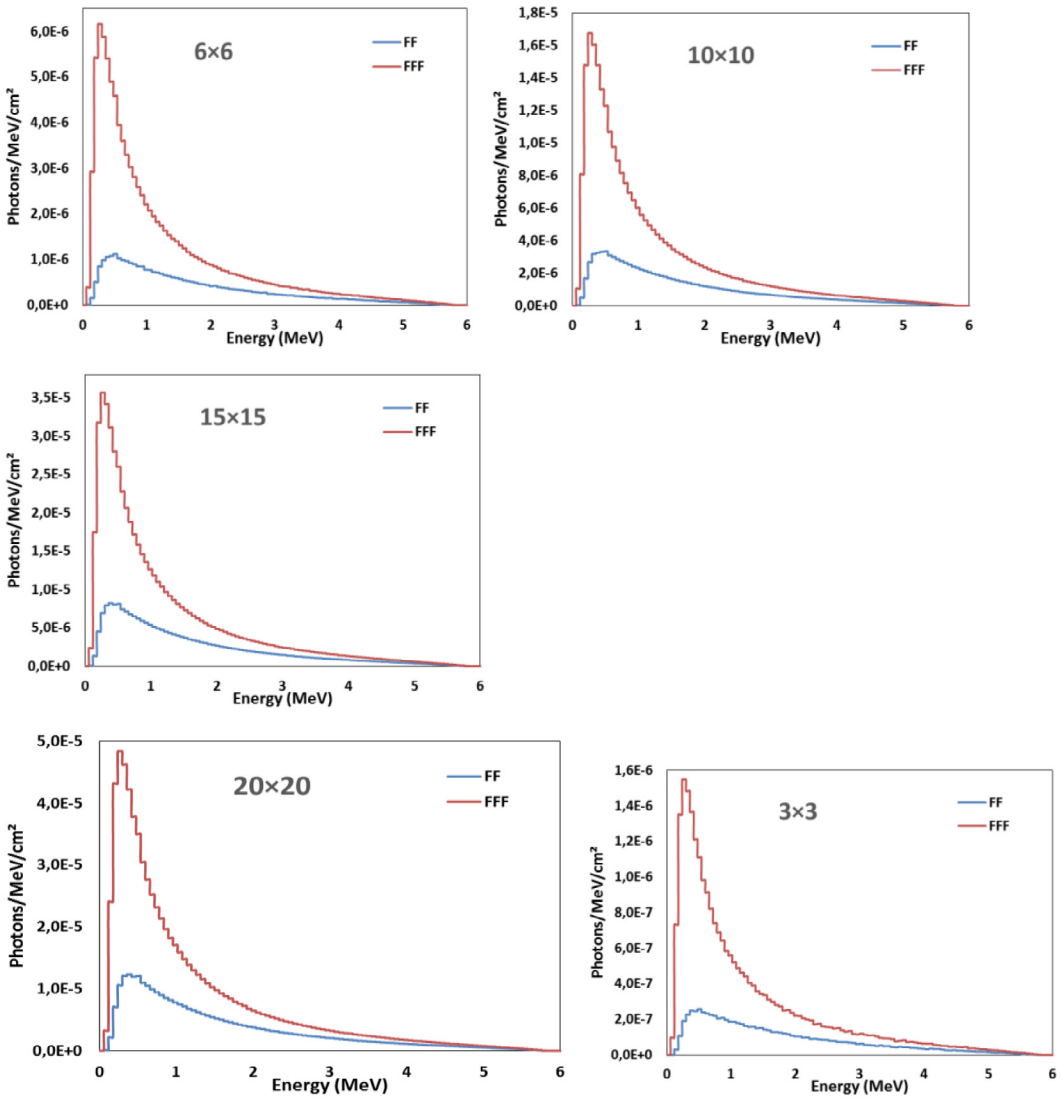


**Figure 8** Comparison of photon beams spectrum of FF and FFF 6 MV photon beams for different field sizes.

**Table 5** Ratio of fluency of initial particles for FFF and FF beam with field size.

| Field size ($cm^2$) | Ratio of photon energy spectra for (FFF to FF) |
|---|---|
| 3 × 3 | 3.76 |
| 6 × 6 | 2.74 |
| 10 × 10 | 2.56 |
| 15 × 15 | 2.36 |
| 20 × 20 | 2.18 |

The photon energy spectra of two configurations FF and FFF beams are shown in Fig. 8. By looking to the Fig. 8, it's clear that the photon energy spectra of FFF beams are higher than FF beams for all field sizes. This is due to the beam attenuation in standard case (FF beams). On the other hand, as it is clear in the Table 5, the differential ratio for FFF to FF beams decreases with a field size, it decreases from 3.76 to 2.19 for 3 × 3 to 20 × 20 $cm^2$ field size, respectively, due to the fixed form of the flattening filter (FF). The results presented in Fig. 4 are compared to the study of Mesbahi (2007), and we noted that there are slightly different due to the results of present paper are calculated in a circle of radius 10 cm at the phantom surface and his calculations were performed over the irradiated field size.

## 4. Conclusion

In this present work, BEAMnrc Monte Carlo model has been applied to simulate a 6 MV photon beam of a Varian Linac with and without a flattening filter. Beam profiles, percentage depth dose, surface dose, out-of-field and head scatter for both FF and FFF beams have been evaluated. The results indicated that removing the flattening filter reduces the penumbra dose, head scatter, out-of-field doses and increases the dose rate and surface dose. The dose rate of unflattened beam was about 2.46 times higher than the flattened beam, clinically, reducing the fraction delivery time with FFF beams. The difference between FFF and FF doses outside the field (at 3.5 cm from the treatment field border) was 40%, 35%, 31%, 20% and 15% for

$20 \times 20$, $15 \times 15$, $10 \times 10$, $6 \times 6$ and $3 \times 3\,cm^2$ field sizes, respectively.

Using the helium particles instead the air column under the jaws, in FFF case, reduces the surface dose, build-up doses and $d_{max}$ restored as in the flattened one. Clinically, the unflattened beam is useful to treating and killing the cancer cells.

## References


Chung, J.-B., Kim, J.-S., Eom, K.-Y., Kim, I.-A., Kang, S.-W., Lee, J.-W., Kim, J.-Y., Suh, T.-S., 2015. Comparison of VMAT-SABR treatment plans with flattening filter (FF) and flattening filter-free (FFF) beam for localized prostate cancer. J. Appl. Clin. Med. Phys.

Detappe, A., Tsiamas, P., Ngwa, W., Zygmanski, P., Makrigiorgos, M., Berbeco, R., 2013. The effect of flattening filter free delivery on endothelial dose enhancement with gold nanoparticles. Med. Phys. 40, 031706.

Diallo, I., Haddy, N., Adjadj, E., Samand, A., Quiniou, E., Chavaudra, J., Alziar, I., Perret, N., Guérin, S., Lefkopoulos, D., de Vathaire, F., 2009. Frequency distribution of second solid cancer locations in relation to the irradiated volume among 115 patients treated for childhood cancer. Int. J. Radiat. Oncol. Biol. Phys. 74, 876–883. http://dx.doi.org/10.1016/j.ijrobp.2009.01.040.

Georg, D., Knöös, T., McClean, B., 2011. Current status and future perspective of flattening filter free photon beams. Med. Phys. 38, 1280. http://dx.doi.org/10.1118/1.3554643.

Hrbacek, J., Lang, S., Klöck, S., 2011. Commissioning of photon beams of a flattening filter-free linear accelerator and the accuracy of beam modeling using an anisotropic analytical algorithm. Int. J. Radiat. Oncol. 80, 1228–1237. http://dx.doi.org/10.1016/j.ijrobp.2010.09.050.

Kragl, G., af Wetterstedt, S., Knäusl, B., Lind, M., McCavana, P., Knöös, T., McClean, B., Georg, D., 2009. Dosimetric characteristics of 6 and 10 MV unflattened photon beams. Radiother. Oncol. 93, 141–146. http://dx.doi.org/10.1016/j.radonc.2009.06.008.

Kry, S.F., Titt, U., Pönisch, F., Vassiliev, O.N., Salehpour, M., Gillin, M., Mohan, R., 2007. Reduced neutron production through use of a flattening-filter-free accelerator. Int. J. Radiat. Oncol. 68, 1260–1264. http://dx.doi.org/10.1016/j.ijrobp.2007.04.002.

Lutz, W.R., Larsen, R.D., 1984. The effect of flattening filter design on quality variations within an 8-MV primary X-ray beam. Med. Phys. 11, 843–845. http://dx.doi.org/10.1118/1.595573.

Ma, C.M., Rogers, D.W.O., 2004. BEAMDP as a General-Purpose Utility. NRC Rep. PIRS 509e Rev A.

Maged Mohammed, E., Chakir, T. El, Khoukhi, H., Boukhal, M., Azahra, J. El, Bakkali, Mroan, Saed, A.A., El Bardouni, T., 2015. Dosimetric Properties of the Field Sizes of 12 MV Photon Beams: A Monte Carlo Study. J. Nucl. Particle Phys. 5 (3), 52–57. http://dx.doi.org/10.5923/j.jnpp.20150503.02.

Mesbahi, A., 2007. Dosimetric characteristics of unflattened 6 MV photon beams of a clinical linear accelerator: a Monte Carlo study. Appl. Radiat. Isot. 65, 1029–1036. http://dx.doi.org/10.1016/j.apradiso.2007.04.023.

Mesbahi, A., Reilly, A.J., Thwaites, D.I., 2006. Development and commissioning of a Monte Carlo photon beam model for Varian Clinac 2100EX linear accelerator. Appl. Radiat. Isot. 64, 656–662. http://dx.doi.org/10.1016/j.apradiso.2005.12.012.

Najem, M.A., Spyrou, N.M., Podolyák, Z., Abolaban, F.A., 2014. The physical characteristics of the 15 MV Varian Clinac 2100C unflattened beam. Radiat. Phys. Chem. 95, 205–209. http://dx.doi.org/10.1016/j.radphyschem.2013.04.035.

Pichandi, A., Ganesh, K.M., Jerin, A., Balaji, K., Kilara, G., 2014. Analysis of physical parameters and determination of inflection point for flattening filter free beams in medical linear accelerator. Rep. Pract. Oncol. Radiother. 19, 322–331. http://dx.doi.org/10.1016/j.rpor.2014.01.004.

Pönisch, F., Titt, U., Vassiliev, O.N., Kry, S.F., Mohan, R., 2006. Properties of unflattened photon beams shaped by a multileaf collimator. Med. Phys. 33, 1738–1746. http://dx.doi.org/10.1118/1.2201149.

Rogers, D.W.O., Walters, B., Kawrakow, I., others, 2001. BEAMnrc Users Manual. NRC Rep. PIRS 509.

Sigamani, A., Nambiraj, A., Yadav, G., Giribabu, A., Srinivasan, K., Gurusamy, V., Raman, K., Karunakaran, K., Thiyagarajan, R., 2016. Surface dose measurements and comparison of unflattened and flattened photon beams. J. Med. Phys. 41, 85. http://dx.doi.org/10.4103/0971-6203.181648.

Smathers, J.B., 2003. The physics of radiation therapy. In: Khan, Faiz M. (Ed.), J. Appl. Clin. Med. Phys.. . third ed., vol. 4, pp. 382–383. http://dx.doi.org/10.1120/jacmp.v4i4.2507.

Titt, U., Vassiliev, O.N., Pönisch, F., Dong, L., Liu, H., Mohan, R., 2006. A flattening filter free photon treatment concept evaluation with Monte Carlo. Med. Phys. 33, 1595. http://dx.doi.org/10.1118/1.2198327.

Tsiamas, P., Sajo, E., Cifter, F., Theodorou, K., Kappas, C., Makrigiorgos, M., Marcus, K., Zygmanski, P., 2014. Beam quality and dose perturbation of 6 MV flattening-filter-free linac. Phys. Med. 30, 47–56. http://dx.doi.org/10.1016/j.ejmp.2013.02.004.

Vassiliev, O.N., Titt, U., Pönisch, F., Kry, S.F., Mohan, R., Gillin, M. T., 2006. Dosimetric properties of photon beams from a flattening filter free clinical accelerator. Phys. Med. Biol. 51, 1907–1917. http://dx.doi.org/10.1088/0031-9155/51/7/019.

Walters, B., Kawrakow, I., Rogers, D.W.O., 2005. DOSXYZnrc Users Manual. NRC Rep. PIRS 794.

Wang, Y., Khan, M.K., Ting, J.Y., Easterling, S.B., 2012. Surface dose investigation of the flattening filter-free photon beams. Int. J. Radiat. Oncol. 83, e281–e285. http://dx.doi.org/10.1016/j.ijrobp.2011.12.064.

Wiant, D.B., Terrell, J.A., Maurer, J.M., Yount, C.L., Sintay, B.J., 2013. Commissioning and validation of BrainLAB cones for 6X FFF and 10X FFF beams on a Varian TrueBeam STx. J. Appl. Clin. Med. Phys. 14.

Xiao, Y., Kry, S.F., Popple, R., Yorke, E., Papanikolaou, N., Stathakis, S., Xia, P., Huq, S., Bayouth, J., Galvin, J., Yin, F.-F., 2015. Flattening filter-free accelerators: a report from the AAPM therapy emerging technology assessment work group. J. Appl. Clin. Med. Phys. 16. http://dx.doi.org/10.1120/jacmp.v16i3.5219.

Yarahmadi, M., Allahverdi, M., Nedaie, H.A., Asnaashari, K., Vaezzadeh, S.A., Sauer, O.A., 2013. Improvement of the penumbra for small radiosurgical fields using flattening filter free low megavoltage beams. Z. Für Med. Phys. 23, 291–299. http://dx.doi.org/10.1016/j.zemedi.2013.03.011.